Silicon Micromachined EBG Resonator and Two-Pole Filter With Improved Performance Characteristics

Timo Euler and John Papapolymerou, *Member, IEEE*

***Abstract*—A novel micromachined resonator at 45 GHz based on a defect in a periodic electromagnetic bandgap structure (EBG) and a two-pole Tchebyshev filter with 1.4% 0.15 dB equiripple bandwidth and 2.3 dB loss employing this resonator are presented in this letter. The periodic bandgap structure is realized on a 400 μm thick high-resistivity silicon wafer using deep reactive ion etching techniques. The resonator and filter can be accessed via coplanar waveguide feeds.**

***Index Terms*—Electromagnetic bandgap structures (EBG), micromachining, PBG, planar filter, wireless application.**

I. Introduction

During the last ten years, many studies have proven that periodic dielectric structures can exhibit frequency regions where no electromagnetic waves are allowed to propagate [1]. Based on these studies researchers have recently developed several filtering and diplexing devices both at optical and microwave frequencies [2]–[4]. This letter presents a novel monolithic millimeter-wave resonator and filter at 45 GHz using deep micromachining techniques to fabricate the periodic dielectric structures. The employed EBG structure and defect resonator are similar to the ones used in [4]. The same resonating defect in a rectangular lattice located between the first two bands in $\Gamma - X$ direction is chosen for the design. However, there are several differences in the design: The holes used for the EBG structure in this letter have polygonal shape in order to achieve larger bandgaps with less substrate removal; the surrounding EBG was chosen larger to achieve sufficient confinement of the resonant modes; and the feed-design was changed to a simple slot feed in order to reduce the effect of the feed on the resonator. The resonator and filter were fabricated with a thermocompression bond and the measurements show good agreement with the simulations and provide a 3-dB improvement over the prior state of the art [4].

II. Theory and Design

Fig. 1 shows the two-dimensional (2-D) electromagnetic bandgap (EBG) structure employed for the filter design. The structure consists of air cylinders of polygonial outline inscribed in a circle of radius $r/a = 0.375$ in a silicon wafer

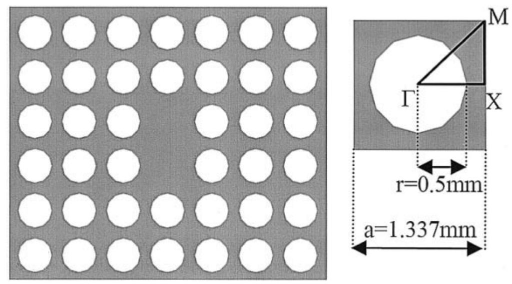

Fig. 1. Two-dimensional periodic bandgap structure employed for the filter design. The air holes in the silicon substrate ($\epsilon_r = 11.7$) are 12-edged polygons inscribed in a circle of radius $r/a = 0.375$, where the lattice constant $a = 1.337$ mm is the distance between adjacent holes. The two missing cylinders comprise the defect resonator used in the filter design.

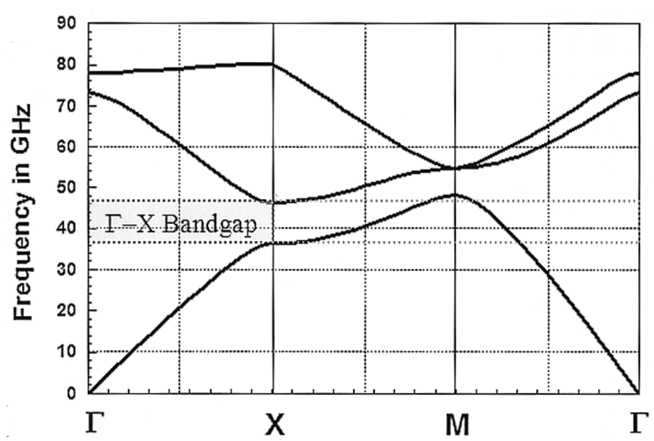

Fig. 2. Bandstructure diagram for the TM-modes of the EBG-structure shown in Fig. 1. The partial bandgap in $\Gamma - X$ direction extends from 36.35 GHz to 46.39 GHz.

($\epsilon_r = 11.7$). The air cylinders are periodically arranged in a rectangular lattice with lattice constant $a = 1.337$ mm and yield an EBG-structure confining the electromagnetic waves in two dimensions. In the third dimension, the structure is bound by metal walls both on its top and bottom confining the electromagnetic waves to TM-modes. The dispersion diagram for the 2-D EBG shows a partial bandgap for the $\Gamma - X$ direction from 36.35 GHz to 46.39 GHz (Fig. 2). A localized defect mode at 44.91 GHz is created by completely removing two cylinders in the lattice. This defect mode constitutes the EBG-defect resonator. Although propagation in the $X - M$ and $M - \Gamma$ direction is allowed for the first band around 45 GHz, the field patterns of the first band do not fulfill the symmetry condition of the created defect mode for those regions. Therefore, no coupling to these modes is observed and the defect mode is truly localized. A higher resonance can be

Manuscript received January 29, 2003; revised June 7, 2003. This work was supported in part by the Yamacraw Design Center of the State of Georgia and in part by the NASA Glenn Research Center under Contract NCC3-900. The review of this letter was arranged by Associate Editor Dr. Rüdiger Vahldieck.

The authors are with School of Electrical and Computer Engineering, The Georgia Institute of Technology, Atlanta, GA 30332-0250 (e-mail: papapol@ece.gatech.edu).

Digital Object Identifier 10.1109/LMWC.2003.817132

observed at 47.25 GHz which is already outside of the $\Gamma - X$ bandgap of the periodic structure.

For larger radii of the cylinders, r/a, the $\Gamma - X$ bandgap opens wider resulting in better spatial confinement of the defect mode. Even a complete bandgap can be realized for $r/a > 0.4$. At the same time, the second resonant mode moves closer to the $\Gamma - X$ bandgap region and strong coupling to it by the external feed can be observed even if it resides in the nonbandgap region. This mode cannot easily be uncoupled as the field distribution is very similar to the one of the localized defect mode. The chosen radius of $r/a = 0.375$ provides sufficient isolation against the second resonant mode.

Creating a defect by removing only a single air cylinder and centering the defect mode in the $\Gamma - X$ bandgap might result in a resonator with better spatial confinement.

In order to fabricate and realize the resonator, the EBG-structure has to be made finite. An extension of the EBG of ten rows to the direction of large spatial extent of the defect mode and five rows to the other direction has been observed to provide enough confinement. The simulations for this resonator show an unloaded Q-factor of $Q_u = 339$ for a 400 μm thick high-resistivity silicon wafer ($\rho_{Si} = 2600\ \Omega$cm) with assumed conductivity of the confining metal layers as $\sigma_{Au} = 4 \cdot 10^7$ S/m.

Access to and from the resonator is achieved via coplanar waveguide feeds. The two-pole filter is designed by using two EBG defect-resonators with the appropriate external and inter-resonator coupling coefficients, Q_{ext} and k_{ij}, according to [5]. For the design of the two-pole filter, a Tchebyshev response with a 1.37% bandwidth, 0.1 dB ripple, and 45 GHz center frequency was selected. This renders the general filter coefficients $g_0 = 1$, $g_1 = 0.843$, $g_2 = 0.622$, and $g_3 = 1.3554$. The required Q_{ext} and k_{ij} can be calculated from the coefficients g_i and the bandwidth of the filter, BW, as follows:

$$Q_{\mathrm{ext}} = \frac{g_0 g_1 \omega}{BW} \tag{1}$$

$$k_{ij} = \frac{BW}{\omega}\sqrt{\frac{1}{g_i g_j}}. \tag{2}$$

In order to achieve the above specifications, the coupling coefficient between the two defects should be $k_{ij} = 0.0189$ and the external Q-factor $Q_{\mathrm{ext}} = 61.6$.

The spacing of the defects and therefore the coupling coefficients k_{ij} can only attain discrete values for a given structure. In order to cover the values in between needed for other filter designs, the radius of the cylinders, r, has to be changed. This can either be done for the complete EBG-structure or only for the holes between the two defects. Changing r for the complete EBG structure can only be done within a certain range, since it changes the properties of the bandgap and the resonator. The desired inter-resonator coupling factor is achieved for a spacing of $6a$ between the defects and $r/a = 0.375$ for the complete EBG-structure.

The external feed was realized by shortening the coplanar waveguide into a slot as shown in Fig. 3. This slot couples to the TM-mode by magnetic coupling. The CPW is designed with a line impedance of 50 Ω at 45 GHz on the 400 μm thick silicon substrate: Its center conductor is $w_{\mathrm{CPW}} = 50\ \mu$m wide and its gap $g_{\mathrm{CPW}} = 30\ \mu$m. Its length is chosen to be $L_{\mathrm{CPW}} = 100\ \mu$m so it is large enough for use of the CPW probes for measurements, but small enough, so the metal cover on top of the structure need only have a small opening for the access port. The end gap was chosen as $G_{\mathrm{CPW}} = 50\ \mu$m.

In order to achieve the desired Q_{ext}, the length, width, and the location of the coupling slot can be adjusted continuously. The width of the slot was fixed at $w_{\mathrm{slot}} = 0.05 \cdot a = 66.85\ \mu$m. The length of the slot, l_{slot}, and the offset off the center of the resonator, o_{slot}, were adjusted to achieve the desired value of Q_{ext} as well as an even shape of the response.

The complete filter was simulated and optimized with Ansoft's HFSS code that is based on the finite-element method (FEM). The simulation result in Fig. 4 shows a ripple of 0.097 dB, a bandwidth of 1.34% and a midband insertion loss of 1.94 dB (due to conductivity losses and imperfect confinement by the finite EBG). The next higher resonance can be seen in the filter response around 47 GHz with a coupling below −18.5 dB. The final dimensions of the filter are 3.61 cm × 1.61 cm.

III. Fabrication

For the fabrication of the resonator and filter, standard IC fabrication techniques along with deep reactive ion etching (RIE) are used. The structure consists of three separate silicon substrates as shown in Fig. 5. The middle piece has the metalized EBG pattern with the coplanar waveguide port openings plated on its top and is micromachined with a deep RIE technique. The middle wafer is 400 μm thick and has a resistivity of $\rho_{Si} = 2600\ \Omega$cm after the etching process. Access windows for RF probing are etched into the top wafer by wet etching with TMAH. The top and bottom silicon pieces are metalized on its bottom and top, respectively, and bonded to the middle piece by a thermocompression bonding process using an SB-6 bonder from Karl Suss to provide the metal shielding of the EBG-structure. The thermocompression bond was done at 320° in nitrogen atmosphere. The pressure was ramped to 2000 mbar during 20 min and applied for 70 min.

IV. Results

The resonator and filter were measured with an Agilent 8510C network analyzer and 50A-GSG-150-VP probes from GGB Industries for contacting the coplanar waveguide feed of the filter. The network analyzer and the probes were calibrated to the GGB CS-5 substrate (50 Ω) employing an SOLT calibration.

The resonant frequency of the fabricated single resonator (and therefore also the fabricated filter) is offset by 3.2% and the measured Q_u is 308 (see Fig. 6). The general shape of the measured filter response matches the simulation very well, but shows slightly higher insertion loss (see Fig. 4). The filter has 20 dB of isolation at 4.1% away from the center frequency. The resonator and filter characteristics of the simulations are compared with the measurements in Table I.

The slightly lower Q-factor and the higher insertion loss is due to the degradation of the resistivity of the silicon in the

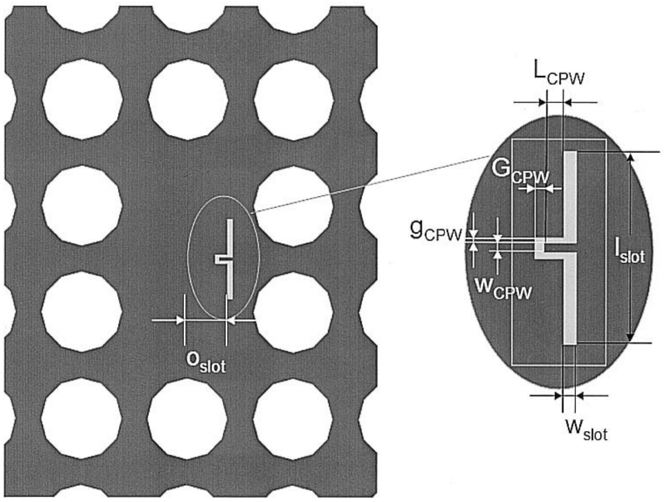

Fig. 3. Geometry of feed slot with offset of the center of the defect, o_{slot}, width of the slot, w_{slot}, length of the slot, l_{slot}, center conductor width of the coplanar waveguide (CPW), w_{CPW}, gap width of the CPW, g_{CPW}, end gap for the CPW, G_{CPW}, and length of the CPW, L_{CPW}.

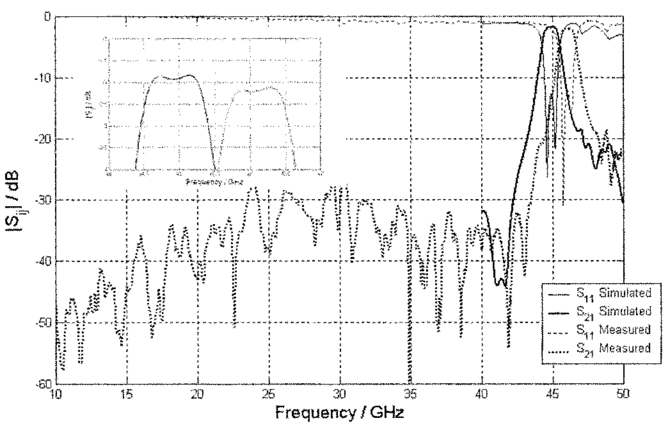

Fig. 4. S-parameters by simulation with Ansoft HFSS and measurements for the two-pole Tchebyshev filter with a zoom on the equiripple region. The simulated 0.097 dB equiripple bandwidth is 1.34% and the midband insertion loss 1.94 dB. The measurements show a 0.15 dB equiripple bandwidth of 1.4% and a midband insertion loss of 2.3 dB.

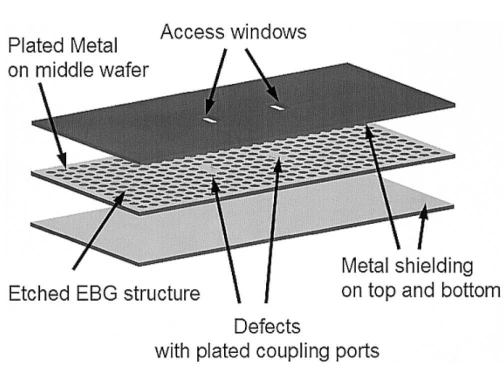

Fig. 5. Schematic picture of the final two-pole coupled EBG-resonator filter.

bonding process, which was not taken into account in the simulations for the filter. The measured resistivity of the wafer after

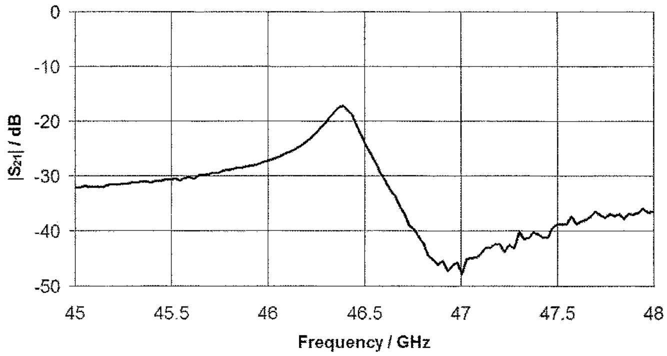

Fig. 6. Measured S_{21}-parameter for the single resonator. The resonant frequency, $f_{\mathrm{resonance}}$, is 46.385 GHz and the unloaded Q-factor, Q_u, is 308.

TABLE I
COMPARISON OF SIMULATED AND MEASURED RESONATOR AND FILTER CHARACTERISTICS

	Simulated	Measured
Q_u	339	308
$f_{resonance}$	44.94 GHz	46.385 GHz
Equiripple	0.097 dB	0.15 dB
Bandwidth	1.335%	1.4%
Insertion loss	1.936 dB	2.3 dB

the bonding process is about $\rho_{Si} = 1100\ \Omega$cm. As the Q-factor and insertion loss are affected only slightly by the higher dielectric conductivity losses, the confinement of the resonant mode by the metal layers and the surrounding EBG-structure is shown to be the limiting factor for the Q-factor. The fabricated holes were slightly larger than the simulated ones, resulting in the frequency offset of the response.

V. CONCLUSION

A micromachined dielectric EBG-defect resonator with measured unloaded Q-factor of 308 and a two-pole Tchebyshev filter at 45 GHz with 1.4% 0.15 dB equiripple bandwidth and 2.3 dB loss employing this resonator are designed and fabricated. The measurements show very good agreement with the simulations and provide a 3-dB improvement over the prior state of the art.

REFERENCES

[1] J. D. Joannopoulos, R. D. Meade, and J. N. Winn, *Photonic Crystals*. Princeton, NJ: Princeton Univ. Press, 1995.

[2] W. J. Chappell, M. P. Little, and L. P. B. Katchi, "High isolation, planar filters using EBG substrates," *IEEE Microwave Wireless Comp. Lett.*, vol. 11, pp. 246–248, 2001.

[3] M. Ito, K. Maruhashi, K. Ikuina, T. Hashiguchi, S. Iwanaga, and K. Ohata, "A 60-GHz-band planar dielectric waveguide filter for flip-chip modules," *IEEE Trans. Microwave Theory Tech.*, vol. 49, pp. 2431–2436, Dec 2001.

[4] B. Lenoir, P. Blondy, D. Baillargeat, S. Verdeyme, P. Guillon, E. Zheng, C. Tavernier, and P. Papapolymerou, "A novel planar silicon waveguide filter at 45 GHz based on a periodic structure," in *IEEE MTT-S Int. Symp. Dig.*, Seattle, WA, June 2–7, 2002, pp. 1923–1926.

[5] G. Matthaei, L. Young, and E. M. T. Jones, *Microwave Filters Impedance-Matching Networks, and Coupling Structures*. Norwood, MA: Artech House, 1980.